# BEM and FEM Approaches to the Analysis of Negative Skin Friction on Piles

G. Russo[1], L. Di Girolamo[2] and G. Marone[3]
[1,2,3]*Department of Civil, Environmental and Architectural Engineering, University of Napoli Federico II, Napoli, Italy*
*E-mail*: pierusso@unina.it

**ABSTRACT:** Negative skin friction (NSF) may be a relevant problem in the design of piles in soft soils, when significant areas around the piles are loaded at the ground surface. The downdrag on piles is traditionally evaluated by reversing a part of the shaft resistance in an applied load and considering it in the evaluation of a safety factor against a bearing capacity failure. Such an approach is totally inadequate, because NSF is actually a problem of soil-pile interaction. Two methods of analysis of a pile subjected to both an external load and NSF are presented: Boundary Element Method (BEM) and Finite Element Method (FEM). The former method is based on a BEM approach and concentrates non-linearity effects at the pile-soil interface while the latter is a FEM approach using the package PLAXIS 2D. The accuracy of the methods is checked back analysing a well-documented case history of bored piles in soft soils.

**KEYWORDS:** Negative Skin Friction (NSF), Dragload, Downdrag, Boundary Element Method (BEM), Finite Element Method (FEM)

## 1. INTRODUCTION

NSF occurs when a settling soil interacts with a pile. The settlement can be due to surface loading, lowering of piezometric head, the dissipation of excess pore pressure induced by pile installation and earthquake or liquefaction induced compression. Whatever the cause of the settlement, the higher the compressibility of the soil the larger is the significance of the problem. NSF can arise also in case of energy piles in which piles are equipped with heat exchangers and are subjected to thermal loads (Russo et al., 2019a, b).

When a heating cycle is applied to a pile it expands, and any axial deformation will be opposed by shaft restraint at the pile–soil interface. If both ends are free to move minimum displacement will occur at mid-depth, and maximum at the ends. These expansive deformations generate NSF, over the upper half of the pile and a positive skin friction over the lower half. If cooled, the pile will contract, generating positive shaft friction over the upper half and NSF over the lower half (Amatya et al., 2012). These different phenomena could lead to additional compression load, dragload, and pile settlement, downdrag, for end bearing and floating piles, respectively. In the presence of NSF, the expected pile behaviour is characterised by an axial compressive force distribution with a maximum below the top of the pile. In Figure 1 a sketch of the axial load along the shaft of a floating (1b) and an end bearing pile (1a) within a settling soil mass is represented. In Figure 2 the corresponding shear stress distributions are reported. This kind of profiles are typical of the so-called "full slip" response, that applies to cases in which the soil settlement is large enough that full slip occurs along the whole pile shaft, and maximum downdrag load is achieved ($\tau(z)/\tau_{lim}(z) = 1$ along the whole pile shaft). Several studies have focused the attention on the maximum value of the dragload and the depth at which it occurs (neutral point).

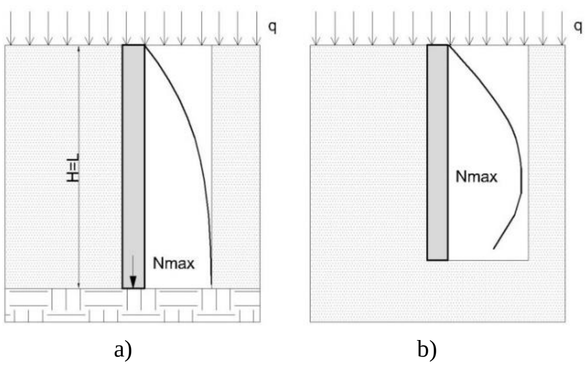


Figure 1 Downdrag force for end-bearing a) and floating piles b)

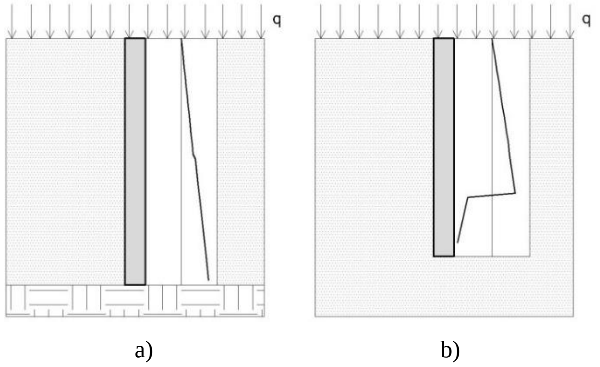


Figure 2 Shear stresses for end-bearing a) and floating piles b)

The traditional design approach is reviewed by Fellenius (1972). NSF $Qs^-$ i.e. the fraction of the lateral resistance mobilised downwards and located in the upper part of the pile (above the neutral point) is considered as an unfavourable load, and the safety factor is evaluated taking into account also the fraction of lateral resistance mobilised upwards below the neutral point, called positive skin friction $Qs^+$. If $Q_b$ is the base resistance, the safety factor FS is:

$$FS = \frac{Q_s^+ + Q_b}{Q_s^- + Q} \quad (1)$$

where Q is the applied head load.

The inadequacy of this approach has been pointed out among others by Alonso et al. (1984) and Franke (1993). As a matter of fact it is easy to recognise that, as long as NSF occurs, a complete failure at the pile-soil interface is impossible, and that the ultimate bearing capacity of the pile is basically not modified by NSF, therefore it is an issue of pile movements and settlement with respect to a settling soil (Tan & Fellenius, 2016).

## 2. EXISTING METHODS

Several methods have been proposed to determine the magnitude and distribution of NSF, including analytical methods and numerical approaches.

Walker & Darvall, (1973) stated that NSF loads on pile can be accurately reproduced theoretically using finite element technique.

Among the analytical methods the majority has been derived by methods which analyse the pile-soil interaction under axial load, adapted to include NSF This is generally achieved by superimposing to the analysis a simplified "free field" soil settlement profile.

The BEM has also been employed among others by Poulos & Davis (1975) with a simplified profile of the settlement of the consolidating ground.

Poulos (2008,2009) has provided a direct approach for piles subjected to NSF, designing the portion of the pile in the stable zone with adequate length and strength.

Ellis (2012) has proposed an alternative approach for the design of piles with NSF. This method allows the capability required in the underlying stable soil to be estimated directly from allowable pile head settlement, soil settlement profile and distribution of shaft stress in the settling layer.

Chen et al. (2009) have provided a modified load transfer method for a pile in nonlinear consolidated soil under different loads at pile top considering the development of shear strength during soil consolidation and loading–unloading scenarios at the pile–soil interface.

Kim et al. (2009) have suggested a simplified method for the analysis of downdrag in single piles using a one-dimensional soil-pile model with the load transfer method combined with the theory of finite strain consolidation.

In numerical modelling both the finite element method (FEM) and the finite difference method (FDM) have been used to investigate the behaviour of a single pile or a pile groups (Liu et al., 2012).

The ground settlements associated with driven piles have been numerically analysed by Indraratna et al. (1992) using axisymmetric FEM employing modified Cam clay theory. The authors have stated that a realistic determination of NSF is primarily dependent on the accuracy of the computed soil and pile settlements.

Jeong et al. (1997) have investigated the pile-soil-pile interaction by using a detailed numerical approach through nonlinear 3D FEM analysis with the computer program ABAQUS.

Lee & Ng (2004) have performed axisymmetric FEM analyses for an end bearing pile, and have reported that the softer the consolidating clay, the greater the difference in the computed dragload from both elastic analysis and slip analysis.

Comodromos & Bareka (2005) have reported the results of 3D analyses on single isolated piles on the effect of the combination of NSF with the application of the working load for single pile and on pile groups finding that dragload group effect is significantly higher for fixed head than free head piles for the practically adopted spacing of 3 diameters.

Hanna & Sharif (2006) have studied the case of single piles driven in clay subjected to axial and surcharge loading through finite element technique combined with the soil responses according to Mohr–Coulomb model .

Liu et al. (2012) have performed finite element analyses of NSF on a single pile, using an axisymmetric model, to study the influence of various influencing factors, including the consolidation time, the pile-soil interface, the lateral earth pressure coefficient, pile-soil limiting displacement, the surcharge, and soil stiffness.

Siegel & Lucarelli (2017) used FDM code FLAC 3D to study the development of NSF for a single pile in settling soil and illustrated that even a small settlement maybe sufficient to develop NSF.

It can be concluded that the existing methods for the analysis of NSF may be grouped in three different categories: (i) those in which both the soil and the pile are modelled as elastic bodies, and the compatibility of displacement is used to couple the two bodies,(ii) those based on empirical approaches as transfer curves (the so called t–z curves), and (iii) numerical modelling as FEM and FDM.

The existing methods of analyses can be also divided in Continuum analyses and Slip analyses. Only the latter methods allow for slip at the pile-soil interface.

Due to the large ground settlement involved in NSF problems, however, the consideration of slip is mandatory for a reliable prediction of pile settlement and downdrag forces.

Elastic methods which do not allow for slip grossly overpredict both figures and maybe considered on the safe side (Jeong & Lee ,2004)

To implement a linear elastic model, an equivalent secant stiffness modulus has to be evaluated.

In a full slip solution, this evaluation is of minor importance since the sensitivity of the results to the stiffness modulus value is rather low.

However, in a pile–soil interaction analysis, the relevant stiffness moduli of the soils involved in NSF calculations are typically large strain moduli.

## 3. THE NEGAT BEM CODE

The method proposed herein for the analysis of piles subjected to NSF is based on the boundary element technique and is implemented into the code NEGAT.

The code is obtained via a modification of the BEM code NAPRA (1998) and it considers floating or end-bearing piles, with diameter varying along the shaft, embedded in a layered elastic continuum and subjected to both axial load and NSF caused by a load of given shape and dimensions in plan and intensity.

The Steinbrenner's approximation is used to account for soil layering (De Sanctis et al.2002).

Both the soil and the pile are modelled as elastic bodies and the compatibility of displacement between the two bodies is retained until a limiting value of the shaft friction is attained.

Both the load at the ground surface and the axial load at the pile head are increased in steps; the intensity of each load step is such to cause the failure of at least one element of the pile-soil interface.

The failure of each element can occur for either positive or NSF; the limiting value of the shear stress at the pile–soil interface is assumed to be independent of the direction.

The limiting value may be either cohesive or frictional; in the latter case the increase in effective stress due to the surface load may be taken into account in the evaluation of the limiting shaft friction.

## 4. COMPARISON WITH EXISTING SOLUTIONS

Several examples of FEM applications to the analysis of NSF on piles are available (Walker & Darvall, (1973), Indraratna et al. (1992), Jeong et al. (1997), Jeong & Lee (2004), Lee & Ng (2004), Comodromos & Bareka (2005), Hanna & Sharif (2006), Liu et al. (2012)).

Some B.E.M. solutions have been published in the form of charts by Poulos & Mattes (1969). Chow et *al.* (1990) used the B.E.M. solutions obtained by Poulos & Mattes (1969) for end-bearing piles, using the "mirror-image technique", to check the accuracy of their own numerical method, based on the solutions by Chan et *al.* (1974).

In Figure 3a the sketch of a pile subjected to NSF for an external loading at the ground surface is reported together with the definition of geometrical and mechanical parameters

In Figure 3b the results obtained by NEGAT are compared to those published by Chow et *al.* (1990) and Poulos & Mattes (1969). The case considered is that of an end bearing pile with a slenderness ratio L/d = 25, and with no slip at the pile–soil interface; the surface load is of infinite width. The Poisson ratio of the soil $\nu_s$ is taken equal to zero, while three different values of the relative pile–soil stiffness $K = E_p/E_s$ have been considered.

The agreement among the different solutions is rather satisfactory.

## 5. FACTORS CONTROLLING NEGATIVE SKIN FRICTION

Elastic solutions show that the pile settlement and the downdrag force induced by NSF depend on the dimensionless parameters L/d, K and the ratio between the Young's modulus of the soil beneath the pile base, $E_b$, and along the shaft, $E_s$ (Poulos & Davis, 1980).

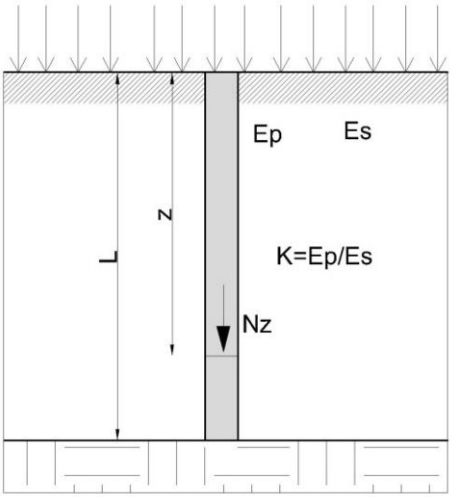


Figure 3a Geometric and mechanical characteristics

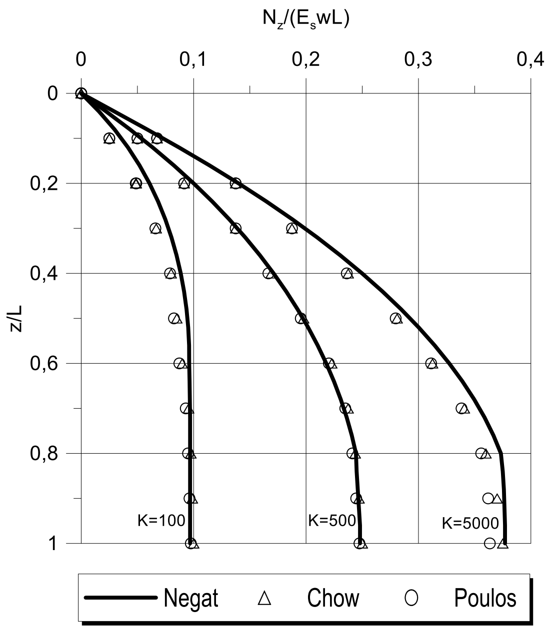


Figure 3b Comparison of Negat (BEM) with Poulos & Mattes (1969) and Chow et al (1990)

Even without any slip at the pile–soil interface, the settlement and downdrag force are significantly affected by the dimensions in plan and intensity of the surface load causing negative friction. While this remark may seem obvious, almost all the methods developed and the parametric studies reported in literature deal with settlement profiles caused by surface load with infinite dimensions in plan. Figures 4 and 5 which are plots based on the results of sensitivity analyses carried out by using Negat code, provide some insight on this factor.

The dimensionless value of the maximum downdrag force along the shaft of a floating pile are plotted in Figure 4 against the ratio B/L, where B is half the size of the square loaded area at the surface. Different load intensity q are considered.

In Figure 5 the same study is repeated for an end-bearing pile. For both the piles the limiting shaft friction is assumed to be purely frictional.

It may be seen that a "full slip" condition is attained for the floating pile at $q/\gamma L = 0.1$; for the end bearing pile, on the contrary, full slip has not yet been attained. Poulos (1989) claimed that "full slip" is likely to occur for values of $q/\gamma L > 0.3 - 0.5$; the results reported in Figures 4 and 5 seem to indicate that this statement applies only to end-bearing piles.

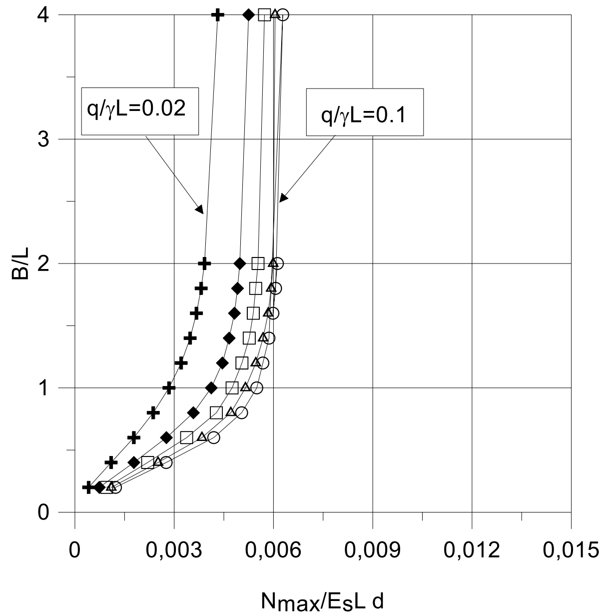


Figure 4 Maximum downdrag in a floating pile

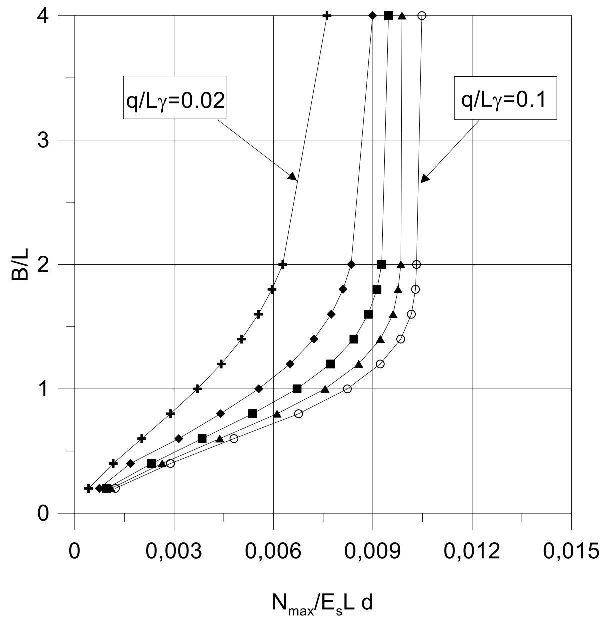


Figure 5 Maximum downdrag in an end-bearing pile

The width of the loaded area, as expressed by the ratio B/L, influences the values of the maximum downdrag force at least until a value of B/L = 1.5 is achieved.

The following general guidelines to a correct choice of the parameters in a negative skin friction analysis can be given:

a) in a layered soil profile, the ratio between the stiffness of the different layers is more important than their absolute value.

This is particularly true if the average pile-soil relative stiffness, K, is higher than 1000 - 2000, which is likely to be the case since negative skin friction usually involves soft soil;

b) the size in plan of the surface load causing the NSF should be taken into account, at least when this width is smaller than 3 - 4 times the embedded length of the piles;

c) the limiting shaft friction should be carefully assessed because the computed values of both the maximum downdrag load and the pile settlement are sensitive to its value, if the pile-soil slip is allowed for.

## 6. A CASE HISTORY OF NEGATIVE SKIN FRICTION ON BORED PILES

The majority of the case histories of NSF reported in the literature refer to driven steel piles. This is mainly due to the use of strain gauges glued or welded on the surface of the steel piles before driving. The most likely reasons of the lack of data about NSF on bored cast in situ piles is the difficulty of the measurements. The probability of damaging the strain gages during the concreting of the pile shaft is quite high (Russo, 2004). Furthermore, the curing of the concrete induces volume changes and hence axial strains which increase, at a decreasing rate, for a long time after the pile installation. Indeed, if the development of NSF is slow, measured strains cannot be easily interpreted due to the overlapping of the two different phenomena.

The NSF case history presented by Picarelli & Sapio (1979) and referring to two bored piles in pyroclastic loose and remoulded silty sand is therefore very valuable, and it is particularly suited for back analysis because of the large amount of informations provided by the Authors in several papers.

### 6.1 Layout of the experimental site.

The layout of the experimental site is reported in Figure 6. The two bored piles were installed at a spacing of about 40 m. The pile A was bored by rotary drilling using bentonite to support the borehole. It was 1 m in diameter and about 21.6 m in length, socketed in a volcanic tuff layer for a length of 2.6 m. The pile B was installed by percussion boring within a casing pipe used to support the borehole. It was 0.8 m in diameter and had approximately the same length of the pile A.

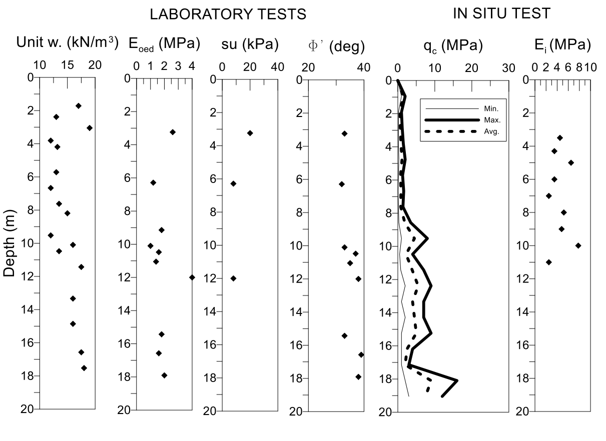


Figure 6 Laboratory and in-situ investigations

At both sites a surface fill was placed between 4 and 7 months after pile concreting, in an attempt to reduce the overlapping between the shrinkage of the concrete due to its curing and the deformations due to the drag load. Three settlement plates at ground surface below the fill, plus a couple of borehole extensometers were used for the purpose of monitoring the settlement at the surface and in depth.

The axial strain was measured at five locations along the shaft of the piles by installing in each section two vibrating wire strain gages; the downdrag load was backfigured by the axial strain and the pile stiffness. The measurements covered a period of about three months at each pile location. Later on, the fill was removed and the piles load tested (Picarelli personal communication).

### 6.2 Site and laboratory investigations

The subsoil at the test site is rather uniform in the horizontal direction and consists of a first layer of pozzolana (volcanic ash and pumices) with organic matter diffused into the mass or interbedded as thin layers of peat, down to a depth of about 10 m below the ground surface. Between the depths of 10 and 14 m the pozzolana is free from organic matter, and from 14 m down to the bearing layer at 19 m calcareous silts and pozzolana are again found. The bearing layer consists of fractured volcanic tuff and has a thickness of at least 5 - 6 m.

The results of soil investigations are reported in Figure 7. The low values of the unit weight (on average 14-16 kN/m$^3$) is typical for both the volcanic and the organic soils. The compressibility of the soils is rather high; the oedometer moduli, $E_{oed}$, at the stress level relevant to the problem, ranges between 0.5 and 2 MPa. The average undrained shear strength by UU triaxial tests on the fine-grained material is about 8-10 kPa but is referred to small lenses of peats which do not have large importance in the problem. The angle of friction is rather high, probably due to a significant sand fraction and to the fibrous structure of the organic matter. The CPT cone resistance qc and the Young's moduli Ei deduced by the self-boring pressuremeter test, are reported in the same figure.

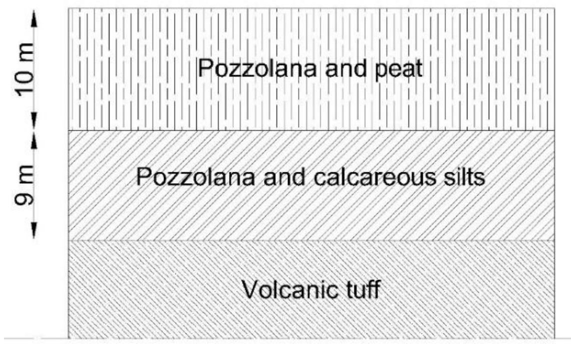


Figure 7 Subsoil model adopted for the back-analysis

### 6.3 Subsoil model

The observed behaviour of the two bored piles, under axial load and in the stage where NSF developed, will be analysed within a single framework. The analysis is aimed not only to check the accuracy of the proposed method, but also to elucidate the importance of some parameters in the predictions.

The subsoil model adopted is reported in Figure 7. The basic choice was to keep the geometry as simple as possible; for this reason, three main layers have been identified. The first is a highly compressible layer of interbedded pozzolana and peat down to a depth of 10 m. The second is a stiffer layer of pozzolana with lower organic content and calcareous silt from 10 m to 19 m. The third is a quite stiff layer of fractured volcanic tuff, with a thickness of at least 6 m. Table 1 gives the average physical and mechanical properties of the three layers.

Table 1 Physical and mechanical properties of the three layers

| Layer depth | γ' (kN/m³) | ϕ' (°) | c' (kPa) | E (kPa) |
|---|---|---|---|---|
| 0 - 10 | 4 | 33 | - | 1500 |
| 10 - 19 | 7 | 37 | - | 2000 |
| 19 - 25 | - | 27° | 300 | 200000 |

Uniaxial compression tests were carried out on the volcanic tuff to determine its compressive strength. Other properties have been assumed on the basis of local experience and taking into account the fractured nature of this soft rock.

In Figure 8 the measured load-settlement relationships obtained via a Maintained Stage Load Test (Russo, 2013) are plotted as full lines. Besides the settlement of the pile head (Figure 8a), the settlement at mid shaft length are also plotted (Figure 8b); they have been calculated by the writers subtracting from the head settlement the shortening of the upper half of the shaft.

In spite of its smaller diameter, the response of pile B, is stiffer than that of pile A; furthermore, pile A exhibits a large residual displacement at unloading. According to Picarelli & Sapio (1979)

### 6.4 Pile load tests

The piles A and B were load tested up to a maximum head load of about 2.1 MN.

this is due to some drilling remains, sedimented at the base of pile A and nullifying the base resistance of the tuff socket substantially making pile A a floating pile. The influence of the technology and of some apparently minor constructional details on the pile performance should never be undervalued (Russo, 2018).

The results of the back-analysis exercise carried out using the NEGAT code are plotted in the same figures by dotted lines; after a trial and error procedure the agreement found is rather satisfactory.

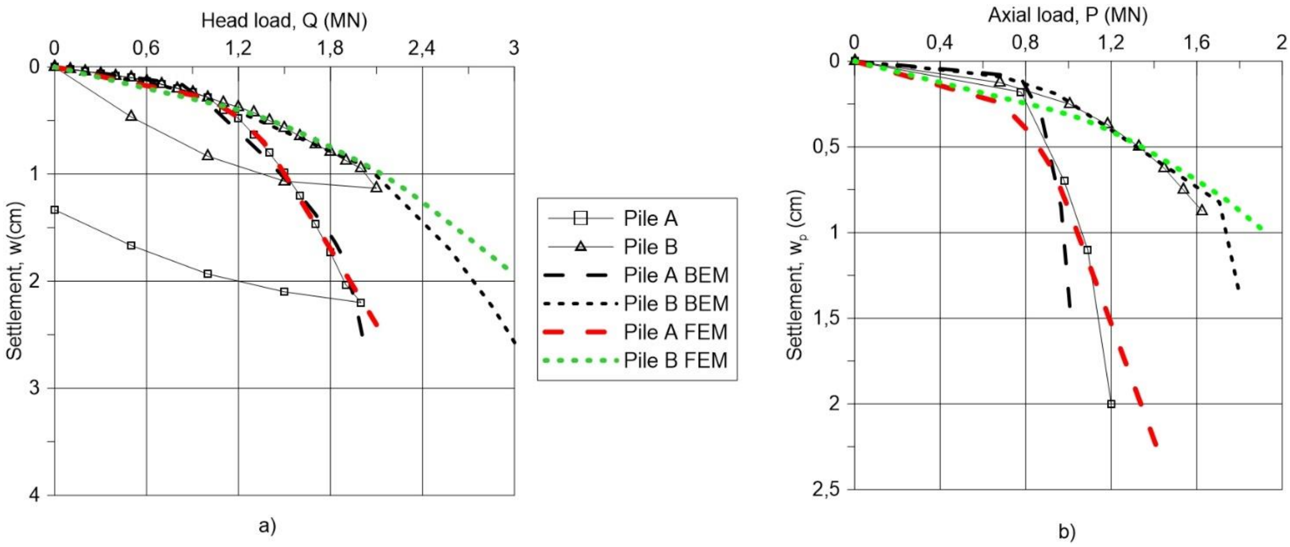


Figure 8 Load-settlement relationship: a) Pile head b) Mid shaft

The parameters which were found to produce the best agreement at the end of the trial and error procedure are listed in Table 2. The procedure was based on several trials where different values of the parameter β and of the base resistance (only for pile B) where tested. The tip resistance of the pile A has been set equal to zero, to simulate the presence of drilling remains sedimented at the bottom of the hole. The skin friction in the socketed part of the two piles has been evaluated on the basis of the suggestions of Carter & Kulawy (1987), taking into account the fractured nature of the tuff; the same value has been found for the two piles (Russo & Marone, 2018). For the upper part of the shaft, on the contrary, significant differences have been found for the value of the parameter β; they have to be related to the different boring techniques adopted for the two piles.

Table 2 Set of parameters used for back analysis

| Layer depth | $\tau_{lim}$ (kPa) pile A | $\tau_{lim}$ (kPa) pile B | $q_b$ (kPa) pile A | $q_b$ (kPa) pile B |
|---|---|---|---|---|
| 0 - 10 | 0.26 $\sigma'_v$ | 0.52 $\sigma'_v$ | - | - |
| 10 - 19 | 0.29 $\sigma'_v$ | 0.58 $\sigma'_v$ | - | - |
| 19 - 25 | 90 | 90 | 0 | 2000 |

### 6.5 NSF with BEM code NEGAT

In Figure 9 the settlement measured at the ground surface as a result of the construction of the embankment around pile A is reported. The embankment has been constructed in two steps, each corresponding to 3.6 kPa; the final ground settlement are respectively 22 and 78 cm, and develop in a relatively short time. The same strategy was followed during the experiment on pile B, using different fill heights corresponding to 3.6 kPa and 5.4 kPa respectively. The final, long term, pile head settlement was recorded only for pile A. It was found to be about 2.5 cm at the first load step and about 5 cm at the final one. This finding confirms that pile A was not really an end-bearing pile, probably due to drilling remains at the bottom of the hole.

In Figure 10 the downdrag load along the shaft, calculated via the strain gages measurements, is plotted vs. the depth. For the sake of briefness, only the first load step of the pile A and the second load step of the pile B are considered. Adjacent to the graphs a sketch of the piles with the strain gage location is reported, outlining the damaged gages.

The back analysis of the downdrag forces and settlement induced by NSF on the piles has been carried out by NEGAT using the same set of parameters obtained by the load tests and listed in Table 1 and 2 but with two different assumptions: i) prediction 1, the limiting shaft friction is evaluated on the basis of the litostatic stress, ii) prediction 2 the limiting shaft friction is evaluated taking into account also the increase in vertical stress due to the fill load. The results obtained are reported in Figure 10 respectively with the label prediction 1 and prediction 2.

The maximum downdrag load calculated for pile A is about 750 kN at the depth of 17 m with the assumption (1) while with the assumption (2) the maximum value is 900 kN at a depth of about 15 m. The calculated settlement of the pile is about 2 cm in the case (1) and 2.4 cm in case (2). The predicted settlement at the ground surface due to the fill load is about 25 cm. The maximum measured downdrag for pile A in the first stage of filling is about 550 kN. It is worth pointing out that such a value does not necessarily

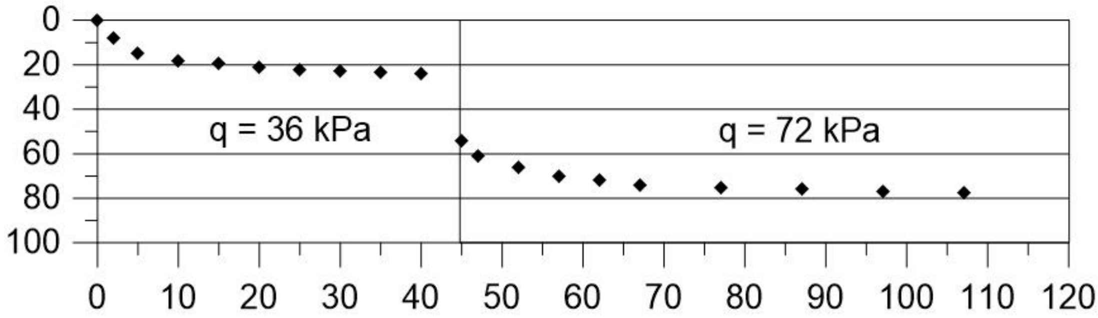


Figure 9 Settlement measured at the ground surface around pile A

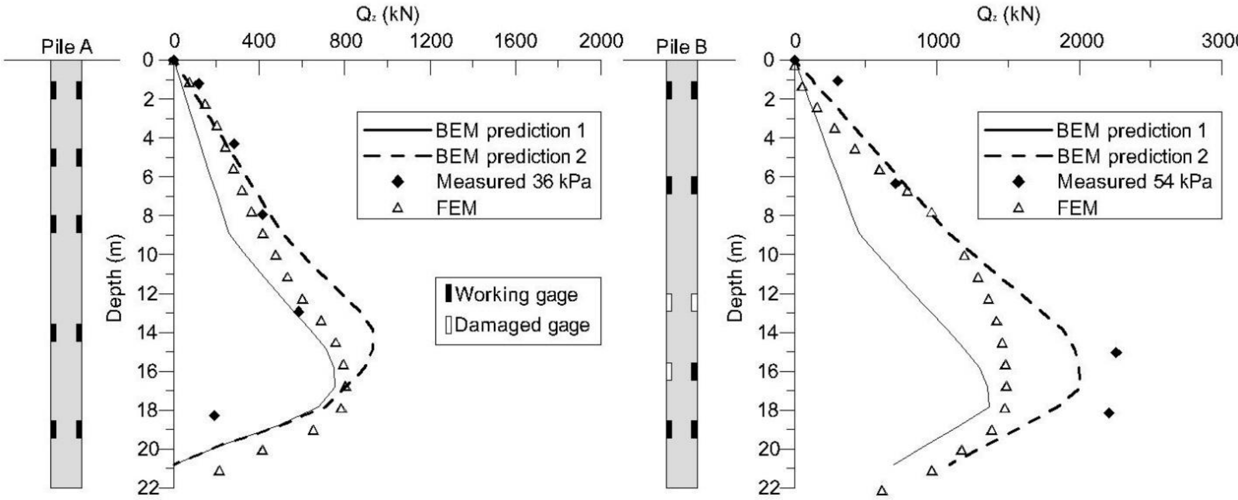


Figure 10 Measured and predicted downdrag load in pile A and pile B
(Prediction 1 and 2 via BEM Code NEGAT, FEM via Plaxis 2D)

represent the actual maximum downdrag load acting on the pile, due to the limited number of measuring points. As a matter of fact, an overall comparison of the calculated and measured values along the shaft shows a reasonable agreement, the prediction 2 being closer to the observed behaviour in terms of both the maximum downdrag load and of the pile head settlement. For the pile B the comparison refers only to the downdrag force. Also, in this case the option (2) seems to provide a better agreement with the observed behaviour.

### 6.6 NSF with FEM MODEL

The case history described in the previous paragraphs is back-analysed also using the FEM package PLAXIS 2D. An axisymmetric model with fine triangular mesh of 15-noded is used to discretise the pile and the soil. The piles are considered to be linearly elastic, while the surrounding soil is idealized as an elasto-perfectly-plastic material with Mohr–Coloumb yield criterion and constant stiffness modulus.

The subsoil properties are the same used in the code NEGAT (Table 1).

Picarelli & Sapio (1982) reported that the residual strength does not differ significantly from the peak one; for this reason a dilatancy angle equal to zero is assumed.

Compatible interface elements with five node pairs are used to simulate the pile–soil interaction in order to allow slip at the pile-soil contact. Constitutive law and friction angle of the interface elements are assumed equal to those used for the surrounding soil. The elastic modulus of both piles is equal to 27500 MPa that is the average modulus reported by Picarelli & Sapio (1979) obtained from laboratory tests carried out on concrete samples.

The FEM results in terms of NSF and load settlements curves for the head and mid shaft for both piles, A and B, are compared with both the experimental and the NEGAT results (Figure 8 and Figure 10).

The soil-pile interaction focus is on the NSF observed along the shaft and load-settlement curves, but the full experimental procedure as reported in the section 6 is modelled in the FEM package.

Firstly, the initial state of stresses is defined with a $K_0$ procedure. The adopted values of $K_0$, 0.9 for the pile A and 3.6 for pile B, were obtained via a best fitting procedure.

The presence of soft material at the toe of pile A, already mentioned in the previous sections, is modelled in the FEM including a soft linear elastic socket.

In the Figure 10 FEM and BEM show a similar trend for the NSF. The results obtained from FEM analyses, are in better agreement with the experimental behaviour in the upper part of the pile shaft. From 13 m depth both the methods, FEM and BEM, underestimate the amount of dragload induced by NSF.

For pile B the maximum value of measured NSF is very high and, as reported by Picarelli & Sapio (1979), at least two times greater than the observed value for pile A at the end of the second step of the fill construction. As can be observed from Figure 10, obviously, the results from FEM analyses are more closer to those obtained from prediction 2 of BEM analyses that account for the full increase in vertical stress due to the fill load.

## 7. CONCLUSIONS

Two methods to calculate NSF on piles embedded in layered soil allowing for slip at the pile-soil interface are briefly presented. The former is based on the BEM and is implemented in a computer code while the latter is based on FEM. The BEM code was first used to analyse the influence of the extent in plan of the loaded area at the ground surface which is indeed a relevant factor often neglected in simplified analytical approaches where infinite extent of the surcharge area is typically assumed. The same code was also compared with existing previously published solutions. Finally, a case history of bored piles in pyroclastic soils is presented and used to validate both the BEM code and the FEM capabilities. The comparison between the experimental results and the computed values allow to appreciate some differences between BEM and FEM (i.e. the need for different $K_0$ values). In the case of BEM code two different predictions were indeed compared, the latter one being the more realistic. As a matter fact the introduction of the surcharge effect on the limiting shaft friction (i.e. prediction 2) produces a more satisfactory comparison with both observed and FEM computed behaviour.

## 8. REFERENCES


Alonso, E., Josa, A., Ledesma, A. (1984). Negative skin friction on piles: a simplified analysis and prediction procedure. *Géotechnique*, vol. 34, n. 3: 341-337.

Amatya B.L., Soga K., Bourne-Webb P.J., Amis T., Laloui L. (2012). Thermo-mechanical behaviour of energy piles. Géotechnique, vol. 62, n. 6: 503-337

Carter, J. P., Kukhawy, F. H. (1987). Analysis and design of foundations socketed into rock. *Research Report 1493-4, Geotechnical engineering group, Cornell University*, New York, Ithaca, 1987.

Castelli, F., Maugeri, M., Motta, E. (1993). Modellazione del fenomeno di attrito negativo nei pali. *Riv. It. di Geotecnica*, vol. XXVII, n. 1: 11-27.

Chan, K.S., Karasudhi, P., Lee, S.L. (1974). Force at a point in the interior of a layered elastic half-space. *Int. Journl. Solids and Structures*, vol. 10: 1179-1199

Chow, Y. K., Chin, J. T., Lee, S.L. (1990). Negative skin friction on pile groups. *Int. Journ. Num. Anal. Meth. Geomech.*, vol. 14, n. 2: 75-91.

Chen R.P. Zhou W.H. Chen Y.M. (2009). Influences of soil consolidation and pile load on the development of negative skin friction of a pile. *Computers and Geotechnics* vol 36: 1265-1271.

Comodromos E. L. Bareka S.V. (2005). Evaluation of negative skin friction effects in pile foundations using 3D nonlinear analysis. *Computers and Geotechnics* vol. 32: 210-221.

De Sanctis,L., Russo G., Viggiani C. (2002). Piled raft on layered soils. *Proc. Ninth International Conference on Piling and Deep Foundations*, pp.279-286 ISBN 2-85978-358-X Nice.

Ellis E.A. (2012). Briefing: Serveaceability of piles with negative skin friction.Geotechnical Engineering vol 166 Issue GE1:3-7.

Fellenius, B. H. (1972). Down-drag on Piles in Clay due to Negative Skin Friction. *Can. geotech. journ.* vol. 9, n. 4: 323-337.

Franke, E. (1993). Design of bored piles, including negative skin friction and horizontal loading. *Proc. 2nd Intern. Geothech. Seminar on Deep Foundations on Bored and Auger Piles*, Ghent, 1-4 June 1993: 43-57, Balkema, Rotterdam.

Hanna A.M. Sharif A. (2006). Drag Force on Single Piles in Clay Subjected to Surcharge Loading. *International Journal of Geomechanics* vol 6:89-96.

Indraratna B. Balasubramaniam A. (1992). Development of negative skin friction in soft Bangkok clay *Can. geotech. Journ*, vol 29: 393-404.

Jeong S. Kim S. Briaud J-L. (1997). Analysis of Downdrag on Pile Groups by the Finite Element Method. *Computers and Geotechnics*, vol 21 n.21: 143-161.

Kim, H. J., Mission, J. L. C. (2009). "Negative Skin Friction on Piles Based on Finite Strain Consolidation Theory and the Nonlinear Load Transfer Method". KSCE Journal of Civil Engineering (2009) 13(2):107-115

Lee C. J. Ng C.W.W. M. (2004). Development of Downdrag on Piles and Piles Groups in consolidating soil. *Journal of Geotechnical and Geoenviromental Engineering*, vol (130)9: 905-914.

Liu J. Gao H. Liu H. (2012). Finite element analyses of negative skin friction on a single pile. *Acta Geotechnica*, vol.7: 239-252.

Ng, H., Karasudhi, P., Lee, S.L. (1976). Prediction of negative skin friction and settlement in piles due to fill surcharge. *Geotech. Eng.* vol. 7, n. 1: 25-46

Picarelli, L., Sapio, G. (1982). Downdrag experiences in organic soils. *Proc. Int. Conf. "Past, Present, and Future of Soil Mechanics. A critical analysis"*, Mexico: 129-134.

Picarelli, L., Sapio, G. (1979). L'attrito negativo su di un palo trivellato in terreni prevalentemente organici. *Riv. It. di Geotecnica*, vol. XIII, n. 3: 137-154.

Poulos, H. G., Mattes, N. S. (1969). The analysis of downdrag in end-bearing piles. *Proc. 7th Int. Conf. Soil Mech.*, Mexico, vol. 2: 203-208.

Poulos, H. G., Davis, E. H. (1975). Prediction of downdrag forces in end-bearing piles. *Journ. of Geotech. Eng. Div.*, ASCE, vol. 101, GT2: 189-204.

Poulos, H. G., Davis, E. H. (1980). Pile foundation analysis and design. New York, Wiley, 1980.

Poulos, H. G. (2008). A practical design approach for piles with negative friction. Geotechnical Engineering vol. 161(1): 19-27.

Poulos, H. G. (2009). Discussion: A practical design approach for piles with negative friction. Geotechnical Engineering 162 June 2009 Issue GE3:187-188.

Russo G. (1998). Numerical analysis of piled rafts. *International Journal for Numerical and Analytical Methods in Geomechanics*, vol. 22: 477-493, John Wiley & Sons Ltd., UK, 1998.

Russo G. (2004) Full scale load tests on instrumented micropiles. *Journal of Geotechnical Engineering proc. I.C.E.* vol. 57, GE3, pp. 127-137, 2004 - ISSN:1353-2618

Russo G. (2013). Experimental investigations and analysis on different pile load testing procedures *Acta Geotechnica* ISSN1861-1125, vol. 8 (1) pp. 17-31, doi. 10.1007/s11440-012-0177-4 on line since May 2012

Russo G., Marone G. (2018). Experimental comparison on different pile load testing methods. *Proceedings of DFI-EFFC Int. Conf. on Deep Found. and Ground Improvement: Urbanization and Infrastructure Development-Future Challenges, Rome*.

Russo G. (2018) Analysis and design of pile foundations under vertical load: an overview. pp.52-71. *Rivista Italiana di Geotecnica (Italian Geotechnical Journal)* – vol. LII (2) pp. 20. ISSN:0557-1405 doi:10.19199/2017.4.0557-1405.47

Russo G., Maiorano, RMS, Marone G., (2019a) Analysis of thermo-mechanical behaviour of energy piles. *Geotechnical Engineering Journal of the SEAGS & AGSSEA* Vol. 50No. 3 ISSN 0046-5828

Russo G., Marone G., Maiorano RMS, (2019b) Experimental behavior and numerical analysis of energy piles in dry sand. *Proceedings of the XVII ECSMGE-2019* Geotechnical Engineering foundation of the future, Reykiavik (Sept.,2019)

Siegel C. T. Lucarelli A. (2017). Theory and modelling of negative skin friction on a pile in soil. *The Journal of the Deep Foundations Institute,* vol. 10, Issue 3:135-142.

Tan A. S., Fellenius B.H. (2016). Negative skin friction pile concepts with soil-structure interaction. *Geotechnical Research,* vol. 3, Issue 4: 137-147.

Walker, L. K., Darvall, P. L. P. (1973). Dragdown on coated and uncoated piles. *Proc. 8th Int. Conf. Soil Mech.*, Moscow, vol. 2, part 1: 257-262.